Theoretical investigation of the electronic structure and transport properties of $Na_{1+x}Co_2O_4$

2004 J. Phys.: Condens. Matter 16 6493

(http://iopscience.iop.org/0953-8984/16/36/015)

INSTITUTE OF PHYSICS PUBLISHING JOURNAL OF PHYSICS: CONDENSED MATTER

J. Phys.: Condens. Matter **16** (2004) 6493–6505 PII: S0953-8984(04)80389-8

Theoretical investigation of the electronic structure and transport properties of $Na_{1+x}Co_2O_4$

Xing Gao, John S Tse and Dennis D Klug

Steacie Institute for Molecular Sciences, National Research Council of Canada, Ottawa, ON, K1A 0R6, Canada

Received 5 May 2004
Published 27 August 2004
Online at stacks.iop.org/JPhysCM/16/6493
doi:10.1088/0953-8984/16/36/015

Abstract

The validity of a simple band description for explaining the unexpectedly large thermopower in $Na_{1+x}Co_2O_4$ was investigated. Non-spin-polarized and spin-polarized electronic structures of layered cobalt oxides $Na_{1+x}Co_2O_4$ are studied by means of first-principles density functional theory calculations. The fractional occupancy of Na is described via two approaches—the virtual crystal approximation and the rigid band model. We also found that the band structure of the valence band is very sensitive to the geometry of the CoO_6 'octahedron', and cannot be described by a simple crystal field model. The Seebeck coefficients are calculated from the standard kinetic theory. The calculated thermopower demonstrates the importance of a high density of states close to the Fermi level. The calculated Seebeck coefficient based on the paramagnetic band structure is apparently in good agreement with experimental observation although it has been suggested that spin entropy may dominate the thermopower. However, the calculation failed to account for the observed negative in-plane Hall coefficient.

1. Introduction

Thermoelectric devices have been attracting renewed interest in recent years mainly because these devices can achieve direct energy conversion without any waste products and can function for long times without maintenance. The key characteristic for materials with high thermoelectric power is governed by the dimensionless quantity $ZT = S^2T/\rho\kappa$, where S is the Seebeck coefficient or thermopower, ρ is the electrical resistivity and κ is the total thermal conductivity containing both electronic and lattice contributions. Recently, the layered cobalt oxide Na_xCoO_2 was found to exhibit good thermoelectric performance and has been extensively studied. Terasaki *et al* [1] reported that single-crystal $NaCo_2O_4$ exhibits unusually large thermopower up to 100 μV K^{-1} at 300 K. This is accompanied by an unusually low resistivity of 200 $\mu\Omega$ cm in the direction parallel to the CoO_2 plane. Kenjiro *et al* [2]

measured the thermal conductivity of single-crystal $NaCo_2O_4$ and showed that the value of the figure of merit exceeded unity at 800 K. This observation can be compared to the measurements on polycrystalline samples by Ohtaki *et al* [3], which suggested a fairly high $ZT \sim 0.8$. A practical advantage of $NaCo_2O_4$ is that this compound exhibits high chemical stability at high temperature where most intermetallic compounds such as Bi_2Te_3, $CoSb_3$ and Si–Ge alloys cannot be used. These characteristics suggested that the doped Na_xCoO_2 compounds may be very promising thermoelectric materials.

Another interesting property of $NaCo_2O_4$ is the relatively high carrier concentration in spite of the fact that is an oxide; oxides in general have been regarded as unsuitable for thermoelectric application because of their poor mobility. Terasaki *et al* found that the carrier density (n) of $NaCo_2O_4$ is of the order of 10^{21}–10^{22} cm^{-3} [1], which is two orders of magnitude larger than that of conventional thermoelectric materials. Moreover, the high specific heat coefficient (40–50 mJ mol^{-1} K^{-2}) [4] of (Na, Ca)Co_2O_4 and the finding that the temperature dependence of the resistivity is proportional to T^p where p is 0.67 below 50 K and 1.2 above 80 K, are indicative of a moderately strongly electron correlated system. It has been speculated that strong electron–electron correlations play an important role in the enhancement of the thermopower. Most recently, from the investigation of the thermopower and magnetization in both longitudinal and transverse magnetic fields, Wang *et al* [5] showed that $Na_{1+x}Co_2O_4$ shows behaviour consistent with it being a strongly correlated system in which the spin entropy accounts for almost all of the thermopower at 2 K and a dominant fraction at 300 K. Thermopower measurements [6] for $Na_{1-x}CoO_2$ under various pressures $\leqslant$20 kbar by Rivadulla *et al* also demonstrated the importance of asymmetry in the density of states close to the Fermi energy. In a correlated system, one expects a conductor of low carrier concentration to have a large S because the diffusive part of S is the transport entropy, of the order of k_BT/E_F, where E_F is the Fermi energy. Since the primary role of Na is to donate charge to the CoO_2 framework and adjust the valence state of the Co ions, it is tempting to improve the thermoelectric properties by decreasing the carrier concentrations via different levels of Na doping. Furthermore, according to the proposed 'strong interaction involving a spin configuration' explanation from a generalized Heikes formula [7], the concentration of Na, which will determine the concentration ratio of Co^{3+} and Co^{4+}, would be important for the enhancement of the Seebeck coefficient. It is surprising to observe that in a single crystal of $Na_{1.36}Co_2O_4$ even though the thermopower is very similar to that of $NaCo_2O_4$, the in-plane resistivity [5, figure 1] is five orders of magnitude larger than that of $NaCo_2O_4$ [1, figure 2(a)].

There are two reports on the calculation of the electronic band of $NaCo_2O_4$ performed within a local density approximation (LDA) that employed the virtual crystal approximation to mimic the effects of fractional Na occupancy [8]. From a simple theoretical transport model and assuming that the effective electron scattering time has no energy dependence, a fairly large value of $S = 110\,\mu$V K^{-1} at 300 K was predicted even though the effects of electron correlation were not considered. Incidentally, this predicted value is in surprising good agreement with the observed value of 100 μV K^{-1}. Spin-polarized local spin density approximation calculations were also performed in order to address the possibility of magnetic ordering [8]. It was suggested that the most probable ground state of $NaCo_2O_4$ is ferromagnetically ordered. However, the most recent experimental susceptibility measurements show that $Na_{0.75}CoO_2$ ($\Theta = 166.4$ K) and $Na_{1.36}Co_2O_4$ ($\Theta = 50 \pm 5$ K) [5] are all antiferromagnetically ordered.

To expand on previous theoretical calculations, we examine the validity of the rigid band model. The rigid band model has been widely used in describing doping effects on compounds although it has been pointed out [8] that this model may not be valid for this system. Furthermore, recent study of Pd substitutions on Co sites [9] also suggested that the rigid band model is incompatible with the experimental results. Therefore, we undertake

comparative calculations on Na_xCoO_2 as the prototype compound of this series employing the virtual crystal approximation and the rigid band model for both the paramagnetic and ferromagnetic electronic states. Other Na fractional occupancies are also investigated in an effort to understand the potential effects of spin polarizations.

2. Computational details

The crystal structure of Na_xCoO_2 consists of alternate stacks of highly vacant Na atoms and CdI_2-type CoO_2 sheets perpendicular to the c axis. Na ions are inserted between the CoO_2 sheets with either a trigonal prismatic (β and γ phase) or octahedral (α phase) environment. The packing differs as regards the number of sheets within the unit cell: 2 (γ phase) or 3 (β and α phase). In this work, we mainly focus on the γ phase, which has been extensively studied by experiments. On the basis of the γ-Na_xCoO_2 structure reported by Jansen and Hoppe [10], we fully optimized the structure with Na ions fully occupying the trigonal prismatic sites 2b. Both the unit cell sizes and internal coordinates were optimized. The geometry optimizations were performed using the program VASP employing ultrasoft pseudopotentials within the generalized gradient approximation (GGA). The optimized lattice constants are $a = 2.90$ Å and $c = 10.76$ Å and can be compared with the experimental results of $a = 2.84$ Å and $c = 10.81$ Å. The a axis is overestimated by 2% but the c axis is underestimated by 0.5%. These small discrepancies may be attributed to the assumption of a fully Na occupied structural model whereas it is only half-occupied in the actual crystal structure. The only free internal coordinate parameter in the optimization is the relative height of oxygen atoms, i.e. the rhombohedral distortion of the octahedron. The ideal Co–O–Co bond angle would be 90° for a perfect octahedron. In the optimized structure this angle increases to 95.7° indicating a significant distortion. The calculated angle is slightly smaller than the 98.5° obtained in the previous LDA calculation [8] without volume optimization, but this distortion is very close to the observed structure in $Na_{0.7}CoO_2$ [11]. All the optimized structural parameters were carefully checked by force calculations with the full potential linearized augmented plane wave method (FPLAW), which was used for the calculations of the electronic band structure and the Seebeck and Hall coefficients. The maximum force on the atom site is less than 0.4 eV Å^{-1}. For the virtual crystal approximation calculations the same crystal structure was used without further optimization.

Self-consistent electronic band structure calculations were performed with the all-electron full potential linearized augmented plane wave (FLAPW) method [12]. The exchange–correlation potential is treated within the generalized gradient approximation [13] of the density functional theory. Muffin-tin radii of 1.6 and 2.0 au were used for O and Na(Co), respectively. The wavefunctions, the charge density and the potentials are expanded in terms of spherical harmonics inside the muffin-tin spheres. The cut-off angular momentum (l_{max}) is 10 for the wavefunctions and 6 for the charge density and potentials. The Brillouin zone (BZ) integration was performed by the improved tetrahedron method with 2000 k points in the first BZ. The number of augmented plane waves is more than 100 per atom determined by $R_{mt}K_{max} = 7.5$ au. The fractional occupancies of Na are described by the rigid band and the virtual crystal approximation. In the rigid band model, the electronic band structure is fixed as calculated for the fully Na occupied structure ($Na_2Co_2O_4$) and the position of the Fermi level E_F is shifted to reflect the doping levels. In the virtual crystal approximation (VCA), the Na atom is replaced by a pseudoatom with fractional nuclear charge. The VCA approach allows a self-consistent treatment of the change in the charge densities and carrier densities during the electronic structure calculations.

Transport properties relevant to thermoelectric materials, such as the Seebeck coefficient and the Hall coefficient, can be calculated from the electronic band structures with standard

kinetic theory provided that the relaxation time $\tau(E)$ is known. Fortunately, in most cases $\tau(E)$ does not vary significantly with the energy E at low temperature and can be approximated by a constant value, i.e., isotropic relaxation time approximation. It was found that using this isotropic relaxation time approximation reasonably accurate results were obtained [14, 15].

The transport properties were estimated using the standard kinetic theory described in detail by Ziman [16]. In the low field limit the electrical conductivity of a crystalline metallic solid can be calculated from its band structure using the energy integral

$$\sigma_0(T) = \frac{e^2}{3\hbar}\int \mathrm{d}E\,\tau(E,T)N(E)\upsilon^2(E)\left[-\frac{\partial f(E)}{\partial E}\right] \tag{1}$$

where e, τ, f and υ are the electron charge, electronic relaxation time, the Fermi distribution function and the Fermi velocity, respectively. The Seebeck coefficient is proportional to the electron velocity and the electron density of states convoluted by the Fermi distribution function and can be calculated from the ratio of the zeroth and first moment of the electrical conductivity:

$$S(T) = \frac{1}{eT}\frac{I^1}{I^0} \tag{2}$$

where

$$I^x(T) = \int \mathrm{d}E\,\tau(E,T)N(E)\upsilon^2(E)(E-E_\mathrm{F})^x\left[-\frac{\partial f(E)}{\partial E}\right]. \tag{3}$$

The Hall concentration is given by

$$n_\mathrm{H} = -\sigma^2/e\sigma_\mathrm{H} \tag{4}$$

$$\sigma_\mathrm{H} = \frac{e^3}{6\hbar}\int \mathrm{d}E\,\tau^2(E,T)N(E)\,\vec{\upsilon}\,(E)[\mathrm{Tr}(\vec{M}^{-1}) - \vec{M}^{-1}]\,\vec{\upsilon}\,(E)\left[-\frac{\partial f(E)}{\partial E}\right]. \tag{5}$$

where $\vec{M}^{-1}$ represents the inverse mass tensor.

To evaluate the appropriate integrals, Fermi surface integration is carried out with a very dense k-point mesh with the modified Shankland–Koelling–Wood (SKW) [17] band interpolation scheme [18]. Usually approximately 40 000 k points in the first Brillouin zone were used in the calculations.

3. Results and discussion

3.1. Paramagnetic electronic structures

First, we compare the band structure obtained from the optimized structure with the previous result. At a glance, the band structure of the conduction band appears to be similar but there are severe differences. One of the most apparent differences is that the Fermi level cuts the Co 3d t_{2g} band at four places along Γ–K and forming one ring-like and one pocket-like Fermi surface in previous calculations, but the Fermi level only cuts the Co 3d t_{2g} band twice; thus the ring-like Fermi surface vanishes. In order to explain the discrepancies we repeated the calculation with the same geometry of the CoO_6 octahedron as used in previous calculations and obtained identical results. Therefore, it is apparent that the band structure of the electronic Co 3d band is very sensitive to the local geometry of the CoO_6 octahedron. To examine this effect, we performed a series of calculations by distorting the Co–O–Co angle from the ideal 90°–100°. The results are summarized in figure 1. A comparison of the band structure at 90°–100° shows that the changes in the band dispersion and the Fermi surface are tremendous. At 100° we found that the Fermi surface cuts the Γ–K direction at four places forming a ring and a pocket. This is exactly the same as in previous calculations. However, at the ideal octahedron

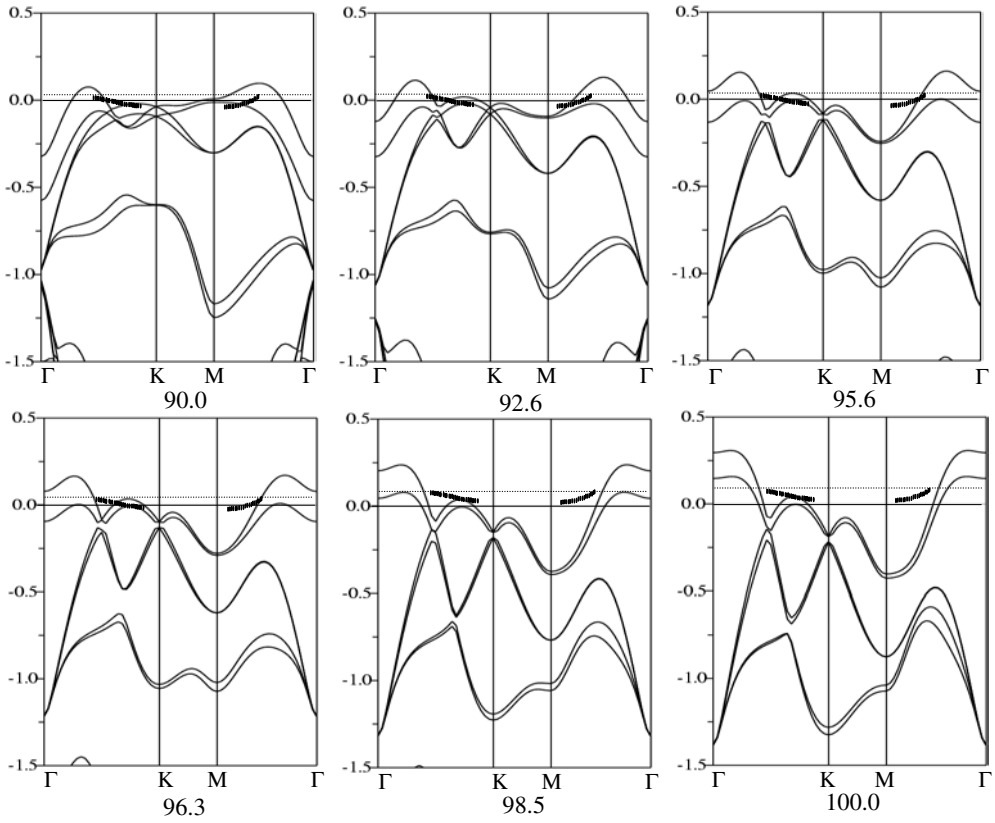

Figure 1. Paramagnetic band structures calculated with different Co–O–Co bond angles for $Na_{0.5}CoO_2$ with experimental lattice parameters within the GGA approximation. The Fermi energy is located at 0. The dotted lines correspond to Fermi levels in $Na_{0.7}CoO_2$ with different doping levels within the rigid band approximation. The rigid band result for $Na_{0.7}CoO_2$ is essentially identical with a virtual crystal calculation for $Na_{0.7}CoO_2$ (not shown). The short thick dotted lines are ARPES measurements from [21].

90°, the Fermi surface only cut the Γ–K direction at two places and the ring vanished. On the other hand, the dispersion is slightly 'flatter' at 90° but becomes very steep at 100°. This is most obvious in the Γ–M direction. The band dispersion of the first two occupied bands is evidently much steeper at 100° than that at 90°.

Secondly, we study the band structure of Na_xCoO_2 as a function of the Na concentration. We employed both the VCA and the rigid band approximation to account for the fractional occupancy in Na_xCoO_2 at the GGA optimized CoO_6 geometry. A comparison of the conduction bands derived from the VCA and rigid band calculations corresponding to the stoichiometry $NaCo_2O_4$ is shown in figure 2. It is evident that the Co dominated valence bands crossing the Fermi surface are very similar. There are, however, some minor but subtle differences. The band dispersion in the VCA calculation is steeper than that in the rigid band model in the A → L and Γ → M directions. Along the L → H → A symmetry line, the Fermi level crosses the band halfway along H → A in the VCA but not in the rigid band. Otherwise, the features in the band are very similar in the two cases. The result shows that the details of the band dispersion are very sensitive to the doping concentrations. A more stringent comparison between the two approximations involves computing the Seebeck coefficient and the Hall

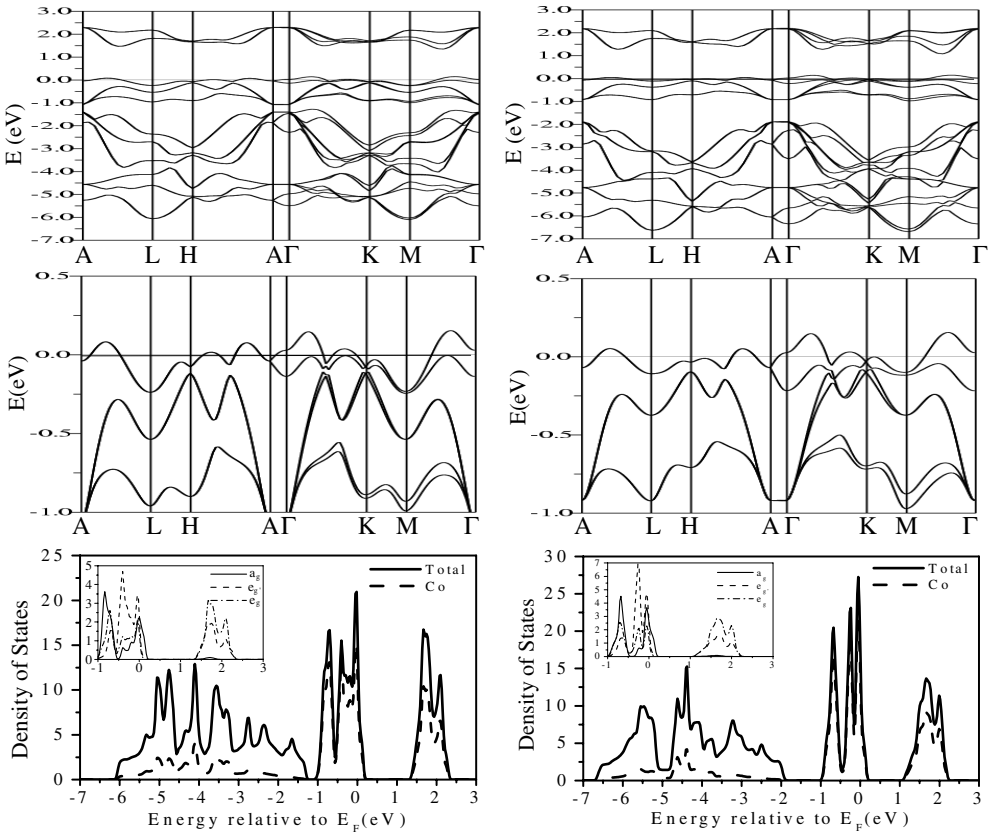

Figure 2. The GGA paramagnetic band structure and density of states (DOS) of $NaCo_2O_4$. Left panel: with the virtual crystal approximation and right panel: with the rigid band model. The middle panel is an enlargement around the Fermi level showing the Co t_{2g} manifold. The solid curve is the total DOS per unit cell while the dotted curve is the projection of the Co d character in the LAPW spheres. The inset shows the Co d partial DOS.

concentration. The two quantities are not only sensitive to the density of states near the Fermi level but also related to the first derivative and second derivative of the Fermi surface. The Hall concentration is particularly sensitive to the band structure as it involves the evaluation of the mass tensor, which is the second derivative of the band dispersion and therefore provides a very sensitive test of the topology of the Fermi surface. The derivatives are numerically difficult to evaluate for 'flat' electronic bands crossing the Fermi level, which are frequently encountered in compounds with large Seebeck coefficient. An accurate description of the curvature of the electronic bands is required.

For an oxide, $NaCo_2O_4$ has a surprisingly high carrier concentration. The electronic band structure can be used to compute the Hall concentration. At the Fermi level, both the virtual crystal and rigid band model predicted a Hall concentration of about 1.6 per unit cell or 0.8 holes per Co ion. This value is to be compared with the earlier LDA estimated value of 0.5 holes per Co ion [8]. The small difference between the present and previous calculations is probably due to the different band interpolation and integration scheme employed. The calculated absolute magnitude of the Hall carrier concentration agrees well with the experimental measurement of 10^{21}–10^{22} cm^{-3}. Furthermore, we found that the Hall concentration is only slightly dependent

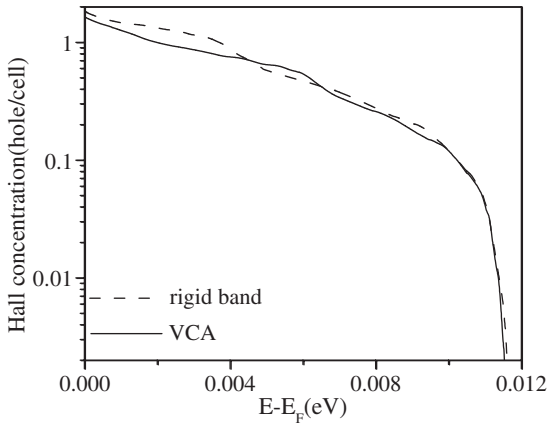

Figure 3. The computed Hall concentration as a function of the energy shift from the Fermi level, $E - E_F$, corresponding to different Na concentrations.

on the doping level. For example, the removal of 0.1 electrons/unit cell the Hall concentration only reduces to 1.4 per unit cell. In figure 3, it is shown that as the doping level increases (p doping), the carrier density decreases. This observation is consistent the experimental observation that the electrical resistivity increases with Na concentration.

It should be noted that the calculations did not give a negative sign of the in-plane component of the Hall coefficient as reported in experiment studies [1, 19]. There are several possible reasons for this discrepancy. First of all, the Hall concentration presented here represents a polycrystalline average and the experimental results are measured within the CoO_2 layer in a single crystal. Second, the approximation of an isotropic relaxation time may be inappropriate. Furthermore, since temperature dependent scattering processes are not considered in this model, the present calculation cannot address the temperature dependence of the Hall coefficient [19].

The calculated temperature dependence of the Seebeck coefficient as a function of the energy shift, $E - E_F$, used to model the Na n doping effect, is plotted in figure 4. The virtual crystal approximation and the rigid band model gave broadly similar results—both for the temperature dependence of the Seebeck coefficient and the doping effects on the Hall concentration. However, there are some discrepancies in the Hall coefficient when the energy shift is small and for the Seebeck coefficient at low temperature and at high doping levels (e.g. $x = 0.4$). These differences can be attributed to the subtle differences between the curvatures of several electronic bands close to the Fermi level, most noticeable along the $\Gamma \rightarrow K \rightarrow M$ direction. The results from the comparative study presented invalidate the speculation that the rigid band model is not suitable for the $Na_{1+x}Co_2O_4$ system. In fact, the results show that both the rigid band model and virtual crystal approximation gave reasonable and almost equivalent results for the Seebeck and Hall coefficients. Moreover, the results show that the numerical interpolation scheme proposed earlier for treating flat bands is reliable. Moreover, it seems that small differences in the band structure between the VCA and rigid band model near the Fermi level do not adversely affect the calculated Hall concentration and Seebeck coefficient.

To explore the discrepancy between the calculated and observed signs for the Hall concentration, we compare the calculated electron density of states and electronic band dispersion with experimental results. The valence band of $Na_{0.7}CoO_2$ has been measured with high energy photoemission spectroscopy [20]. The valence band spectrum shows two

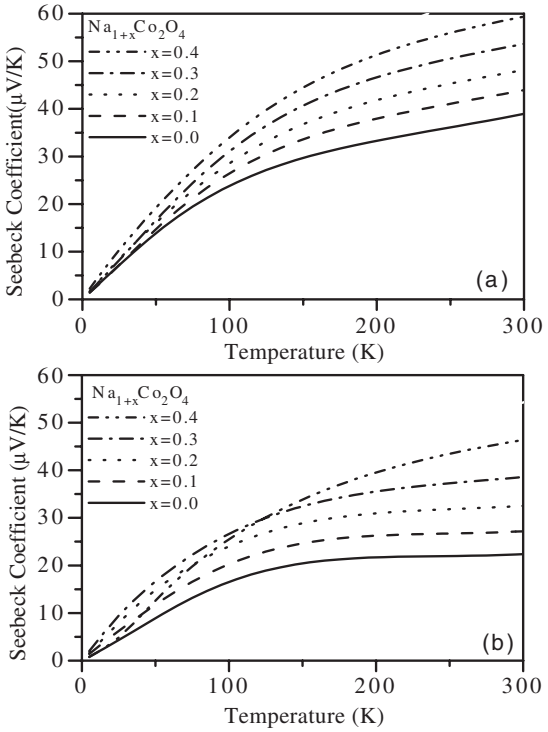

Figure 4. The calculated thermopower as a function of temperature based on the paramagnetic state electronic band structure at different doping levels treated in (a) the virtual crystal approximation and (b) the rigid band model.

bands centred at 1 and 6 eV. The lower binding energy band has a bandwidth of 1.5 eV. The higher energy band is very broad and has a half-width of ∼4 eV. The theoretical densities of states obtained from the VCA and the rigid band model for $Na_{0.5}CoO_2$ shown in figure 2 are very similar. The calculated densities of states are in broad agreement with the observed valence band spectrum. The density of states can be separated into two regions. The lower binding energy region centred around 0.5 eV has a bandwidth of 1 eV. The second region centred around 4 eV from the Fermi level is very broad with a width of 3.5 eV and consists of a series of peaks.

The band dispersions along Γ–K and Γ–M directions for a $Na_{0.7}CoO_2$ sample have been derived from a recent angle-resolved photoemission spectroscopy (ARPES) experiment [21]. As we have commented above, the calculated band dispersions are very sensitive to the distortion of the CoO_6 octahedra. None of the calculated band structures agree quantitatively with the experiment. Under strong rhombohedral distortion—that is, when the Co–O–Co bond angle is 100°—the calculated band structure seems to reproduce the essential features in the experimentally determined Fermi surface. In the experiment, the Fermi surface shows a hole pocket described by two almost concentric circular features centred around the Γ point. The calculation supports this Fermi surface topology. The calculated band dispersion from $\Gamma \rightarrow$ K is in qualitative agreement with experiment. However, even though the predicted dispersion along $\Gamma \rightarrow$ M reproduces the observed form, the calculated dispersion is too steep. As the distortion in the Co–O–Co is reduced to 98.5°, the concentric ring-like feature of the Fermi surface disappears. The calculated band structure gives another pocket along Γ–K in

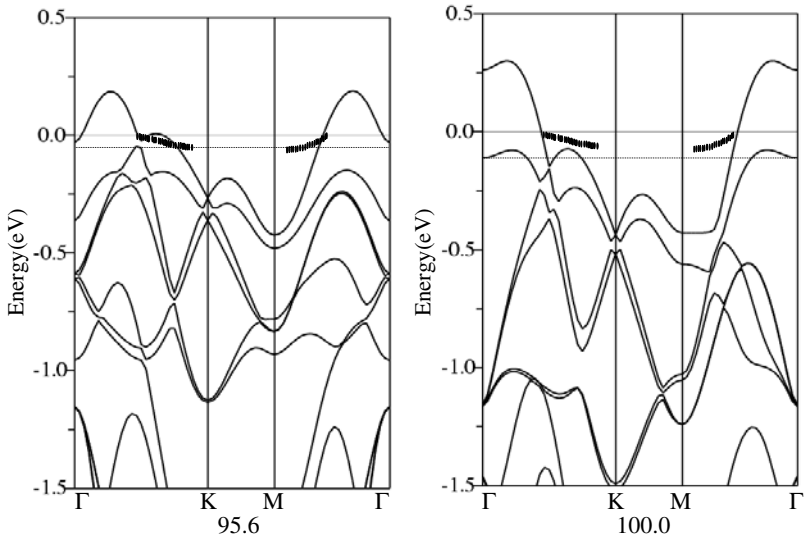

Figure 5. The band structure for Na_xCoO_2 employing the LDA + U approximation. The Fermi level is determined by the rigid band method. The solid curve corresponds to $x = 0.7$ and the dotted line corresponds to $x = 0.5$. The short thick dotted lines are ARPES measurements from [21].

addition to the above hole pocket feature centred around the Γ point. This result is in complete agreement with the previous calculations. The Fermi surface topology remains essentially the same up to a Co–O–Co distortion angle of ∼93°.

Since the Co 3d bands are strongly localized, we investigated the correlation effects using the LDA + U approximation [22]. The calculated band structures for $Na_{0.5}CoO_2$ at Co–O–Co angles of 95.7° and 100° are shown in figure 5. The basic band dispersion topologies from the LDA + U calculations are very similar to the corresponding GGA results. The major difference is that the splitting between the first two conduction bands obtained using GGA is much smaller than that when U is considered. Consequently when U is included, the ring-like Fermi surface is absent in $Na_{0.7}CoO_2$ (using a rigid band shift of the Fermi level) at both distortion angles. For $Na_{0.5}CoO_2$, the ring-like surface remains at a distortion angle of 100° but disappeared at 95.6°. However, unlike the case for the GGA calculations at 100° distortion angle, the LDA + U calculations also predicted a pocket in the $\Gamma \rightarrow$ K direction. Therefore, the LDA + U calculations do not yield significant improvement over the GGA results. We conclude that the Fermi surface topology is very sensitive to both the Na concentration and the distortion of the Co–O–Co angle.

In figure 2, the density of states plot clearly shows the crystal field splittings. Under a rhombohedral distortion, the CoO_6 octahedron is distorted axially and lifts the degeneracy of the sixfold-degenerate t_{2g} band and further splits into a higher energy a_g band and a lower energy e_g' band. The magnitude of this splitting is proportional to the degree of the distortion. The O 2p bands extend approximately from −7.0 to −2.0 eV relative to the Fermi energy E_F and are cleanly separated from the Co d bands. In spite of the 5.7° distortion of the Co–O–Co bond angle (95.7°) from 90° for the ideal octahedron, there is not a resulting clear splitting of the t_{2g} bands (see the Co partial density of states in figure 2). However, close to the top of the band edge where the Fermi level is located, symmetry analysis indeed indicates that it has predominantly Co a_g character. Most recently, Koshibae *et al* [23] pointed out that this shows that the energy splitting of t_{2g} does not originate in the crystal field due to the distortion but is

determined by the kinetic energy of electrons, that is, the electron hopping in a tight binding picture. On the basis of the tight binding Hamiltonian, they suggested that the electronic structures can be described by a Kagomé lattice hidden in the CoO_2 layer in Na_xCoO_2. Their tight binding band dispersion relation captures the first-principles band structure. The essence of the method is that the 3d electron hopping is via the oxygen atoms, indicating significant chemical interactions between Co and the oxygen atoms. In order to further understand this electron hopping contribution, the Mulliken populations are analysed by using an *ab initio* pseudopotential density functional method employing linear combination of numerical atomic orbitals, SIESTA [24][1]. This analysis confirms that there exists strong overlap between Co and O, in support of the proposal of Koshibae *et al*.

The localized nature of the Co d bands near the Fermi level results in fairly 'flat' electronic bands with a very large density of electronic states. This is a favourable feature for high thermopower as indicated in equation (1) and explained above. The calculated Seebeck coefficient as a function of temperature and Na concentration for the virtual crystal and rigid band model are compared in figures 4(a) and (b), respectively. At 300 K, the calculated Seebeck coefficient for undoped $NaCo_2O_4$ is 38 and 22 μV K^{-1} from the virtual crystal and rigid band approximation, respectively. The small difference between the two computational models can be attributed to the slightly different band dispersion profiles of the highest occupied bands. For example, the electronic band along $\Gamma \rightarrow$ K is less dispersive (more flat) in the virtual crystal approximation than the rigid band model. Consequently, the Seebeck coefficient is predicted to be higher by the virtual band approximation. In any case, the values calculated here are lower than the previously estimated value of 110 μV K^{-1} at 300 K based on the degenerate limit ($KT \ll E_F$) of the standard kinetic formula, $S/T = (\pi^2 k^2/3e)[\mathrm{d}n\,(\sigma)/\mathrm{d}E]_{E=E_F}$. The estimated value seems to be in very good agreement with the single-crystal data in the CoO_2 (ab) plane [1]. This agreement may be coincidental, as it has already been noted that the simple formula is linear in temperature whereas the experimental trend of the Seebeck coefficient is already slightly non-linear at this temperature. Moreover, the results presented here represent a polycrystalline average and the theoretical result should be compared with measurements on powder samples. In the latter case, the calculated Seebeck coefficients are in semi-quantitative agreement with experiments on powder samples [4] both in the predicted magnitude and the trend upon increasing Na doping as well as the temperature dependence. The experimental observation that the Seebeck coefficient increases with increasing level of Na doping is well reproduced [1, 4]. For example, the experimental Seebeck coefficient of $Na_{1+x}Co_2O_4$ ($x = 0.1$) at 300 K is 50 and $\sim$56 μV K^{-1} when $x = 0.4$. The calculated value for $x = 0.4$ is 59 μV K^{-1} using the virtual crystal approximation and 46 μV K^{-1} using the rigid band model. In passing, it should be noted that there are significant inconsistencies between different experimental measurements. A more recent measurement on polycrystalline $NaCo_2O_4$ gave a higher Seebeck coefficient of 80 μV K^{-1}. Finally, we note that, although spin entropy has been suggested as a major contributor to the thermopower in this compound [5], the present first-principles Seebeck coefficient calculations within the constant relaxation time approximation and neglecting the spin entropy contributions give reasonable agreement with the experimental measurements as regards to both the temperature dependence and the doping effects. The theoretical results show that the flat bands due to the localized Co d bands close to the Fermi energy with high density of states are an important factor for the high thermopower in $Na_{1+x}Co_2O_4$. It is possible that the combination of flat bands, high densities of states and spin entropy could result in even greater enhancement of the Seebeck coefficient. It is worth

[1] Troullier–Martin norm conserving pseudopotential and double-zeta plus polarization basis sets are used for this calculation. The resultant overlap population between the nearest Co and O changes from 0.162 to 0.194 as the distortion angle is varied from 90° to 100°.

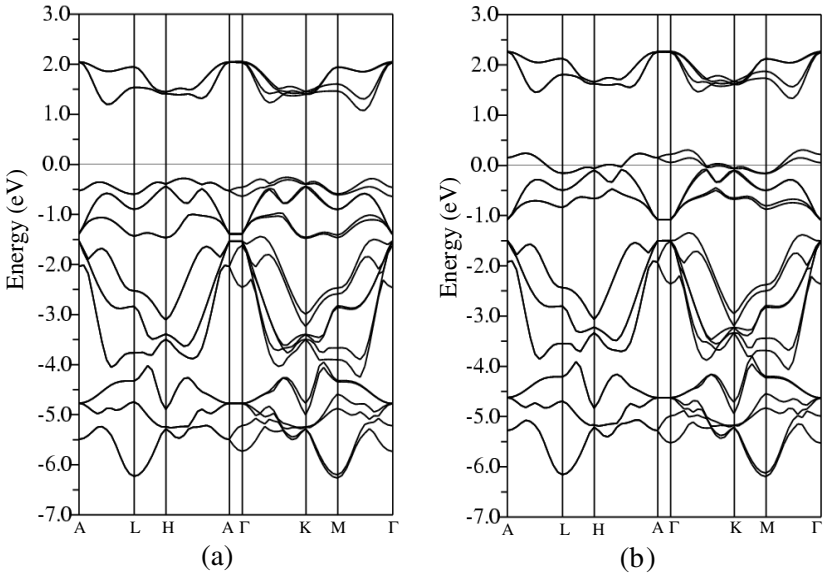

Figure 6. The ferromagnetic band structure of $NaCo_2O_4$.

pointing out that a recent calculation based on the same Boltzmann transport theory of the Seebeck coefficient but using the experimental electronic density of states near the Fermi level obtained from high resolution photoemission spectroscopy also yielded similar results [25]. The calculated thermopower of $Na_{0.6}CoO_2$ reproduces the experimental measurement without the consideration of spin contributions.

3.2. Spin-polarized calculations

To understand in more detail the effects of spin polarization on the electronic structure of $Na_{1+x}Co_2O_4$ we undertake spin-polarized calculations. The electronic states are constrained to ferromagnetic ordering. For a low spin state, if the crystal is restricted to charge neutrality, there can be no spin-unpaired electrons within the rigid band model—the reason being that since $Na_2Co_2O_4$ was taken as the model, all the Co atoms will be in the Co^{3+} valence state and the rigid band model is not applicable. On the other hand, in the virtual crystal approximation, since we adopt half-occupied Na ion sites in the $NaCo_2O_4$ crystal there must be an equal concentration of Co^{3+} and Co^{4+} to satisfy the neutrality condition. The spin-polarized calculations on the ferromagnetic state are consistent with this simple analysis. The ferromagnetic band structure for half-occupied Na ion sites calculated with the virtual crystal approximation is shown in figure 6. When compared to the non-spin-polarized result, the ferromagnetic state is energetically more favourable although the total energy difference is only 79 meV per unit cell. Inspection of the α and β spin density of states indicates that $NaCo_2O_4$ is a half-metal with a spin moment of 1 μ_B per unit cell. In each unit cell there is one spin-unpaired Co d electron. In this case, Co^{3+} has a t_{2g}^6 low spin configuration. The 1 μ_B per unit cell shows that Co^{4+} takes its low spin ($S = 1/2$) state and has a t_{2g}^5 configuration, i.e. a 'hole' in the t_{2g} orbital giving a net magnetic moment of 1 μ_B.

Results of calculations for other fractional Na ion site occupancies with spin polarization are listed in table 1. The Na concentration has a significant effect on the total spin contribution

Table 1. The ferromagnetic solution for $Na_{1+x}Co_2O_4$ with different x, the magnetic moment per unit cell and the total energy difference relative to the paramagnetic electronic state.

x	Magnetic moment per unit cell (μ_B)	Energy (meV/unit cell)
0	1.0	−79.2
0.1	0.9	−67.0
0.2	0.8	−55.3
0.3	0.7	−42.1
0.4	0.6	−30.3

to the magnetic moment of the Co atoms. The results show that higher Na concentrations result in a higher tendency for the Co d electrons to be spin paired. The generalized Heikes formula [7] for the strong interaction case involving spin configuration is

$$S = -\frac{k_B}{e} \ln\left(\frac{g_3}{g_4}\frac{x}{1-x}\right) \tag{6}$$

where g_3 and g_4 represent the numbers of configurations of Co^{3+} and Co^{4+} ions, respectively, and x denotes the concentration of Co^{4+}. For a low spin state, $g_3 = 1$, and $g_4 = 6$. Within this approximation, the Seebeck coefficient is mainly determined by the value of x. In the model proposed in [5], the spin entropy contribution depends mainly on the so-called 'free' spins, which are not antiferromagnetically ordered at low temperature ($T \ll \Theta$, where Θ is the Néel temperature). This indicates that the Na concentration will determine the spin entropy contribution to the Seebeck coefficient. We have not studied the antiferromagnetic state of $Na_{1+x}Co_2O_4$ here. A proper study would require the construction of a larger supercell to account for the antiferromagnetic order for different Na concentrations. The calculation would become more complicated as it would involve full geometry optimization in addition to the computation of the band structure. Such a study will be reported in the future. In this work we focus specifically on the ferromagnetic state of the system. We cannot obtain the spin entropy contributions from the present simple spin-polarized band structure calculations. However, judging from the results of spin-polarized band structure calculations, the magnetic moment is strongly dependent on the Na ion occupancy. For example, in the limit where there are no Na atoms, all the Co atoms would be in the high spin Co^{4+} valence state. In this case, there would be no spin exchange and the spin entropy contribution will be zero. In the other limit, if the Na sites were fully occupied as in α phase ($NaCoO_2$), there would be no net magnetic moment and the spin entropy contribution would diminish. This suggestion, however, is in apparent contradiction with a recent experimental study which showed that the α phase has an even higher Seebeck coefficient. Obviously, more detailed experimental and theoretical studies are needed in order to explain this novel phenomenon.

4. Summary

In this study, we extended previous first-principles calculations on $NaCo_2O_4$ to include the rigid band approximation and the LDA + U to describe fractional occupancy of Na sites. The effects of spin polarization on the electronic structure and the potential relationship of the magnetic moment to the spin entropy contribution to the thermopower are also investigated. It is shown that the rigid band approximation compares well with the virtual crystal approximation for these systems. However, a critical testing of the calculated band structures and Seebeck and Hall coefficients shows that the simple band structure model in the paramagnetic state, either using the rigid band model or the virtual crystal approximation, is not adequate. We found

however that without consideration of the spin entropy, a paramagnetic ground state would yield a high Seebeck coefficient comparable to the experimental observation. We discuss the relative contributions of the spin entropy to the Seebeck coefficient and conclude that optimization of the Na concentration together with the spin entropy contribution may result in a much higher thermopower. We noted that there are several contradictory measurements in the literature that cannot be easily explained by either the simple electronic band or the spin entropy model.

Acknowledgments

We are grateful to Professor T Tritt for useful discussions. This work was supported by a grant from the Office of Naval Research.

References

[1] Terasaki I, Sasago Y and Uchinokura K 1997 *Phys. Rev.* B **56** R12685
[2] Fujita K, Mochida T and Nakamura K 2001 *Japan. J. Appl. Phys.* **40** 4644
[3] Ohtaki M, Nojiri Y and Maeda E 2000 *Proc. 19th Int. Conf. on Thermoelectrics 2000 (Babrow, UK, 2000)* ed D M Rowe, p 190
[4] Ando Y, Miyamoto N, Segawa K, Kawata T and Terasaki I 1999 *Phys. Rev.* B **60** 10584
[5] Wang Y, Rogado N S, Cava R J and Ong N P 2003 *Nature* **423** 425
[6] Rivadulla F, Zhou J S and Goodenough J B 2003 *Phys. Rev.* B **68** 075108
[7] Koshibae W, Tsutsui K and Maekawa S 2000 *Phys. Rev.* B **62** 6869
[8] Singh D J 2000 *Phys. Rev.* B **61** 13397
Singh D J 2003 *Phys. Rev.* B **68** 020503
[9] Kitawaki R and Terasaki I 2002 *J. Phys.: Condens. Matter* **14** 12495
[10] Von Jansen M and Hoppe R 1974 *Z. Anorg. Allg. Chem.* **408** 104
[11] Ono Y, Ishikawa R, Miyazaki Y and Kajitani T 2001 *J. Phys. Soc. Japan* **70** (Suppl. A) 235
[12] Blaha P, Schwarz K, Madsen G K H, Kvasnicka D and Luitz J 2001 *WIEN2k: An Augmented Plane Wave + Local Orbitals Program for Calculating Crystal Properties (Karlheinz Schwarz, Techn. University Wien, Austria)* ISBN3-9501031-1-2
[13] Perdew J P, Burke K and Ernzerhof M 1996 *Phys. Rev. Lett.* **77** 3865
[14] Kim S G, Mazin I I and Singh D J 1998 *Phys. Rev.* B **57** 6199
[15] Tse J S, Uehara K, Rousseau R, Ker A, Ratcliffe C I, White M A and MacKay G 2000 *Phys. Rev. Lett.* **85** 114
[16] Ziman J M 1972 *Principles of the Theory of Solids* (Cambridge: Cambridge University Press)
[17] Pickett W E, Krakauer H and Allen P B 1988 *Phys. Rev.* B **38** 2721
[18] Uehara K and Tse J S 2000 *Phys. Rev.* B **61** 1639
[19] Wang Y, Rogado N S, Cava R J and Ong N P 2003 *Preprint* cond-mat/0305455
[20] Chainani A, Yokoya T, Takata Y, Tamasaku K, Taguchi M, Shimojima T, Kamakura N, Horiba K, Tsuda S, Shin S, Miwa D, Nishino Y, Ishikawa T, Yabashi M, Kobayashi K, Namatame H, Taniguchi M, Takada K, Sasaki T, Sakurai H and Takayama-Muromachi E 2004 *Phys. Rev.* B **69** 180508
[21] Hasan M Z, Chuang Y D, Kuprin A, Kong Y, Qian D, Li Y W, Mesler B, Hussain Z, Fedorov A V, Kimmerling R, Rotenberg E, Rossnagel K, Koh H, Rogado N S, Foo M L and Cava R J 2003 *Preprint* cond-mat/0308438
[22] Anisimov V I, Solovyev I V, Korotin M A, Czyzyk M T and Sawatzky G A 1993 *Phys. Rev.* B **48** 16929
[23] Koshibae W and Maekawa S 2003 *Phys. Rev. Lett.* **91** 257003
[24] Ordejón P, Artacho E and Soler J M 1996 *Phys. Rev.* B **53** 10441
[25] Takeuchi T, Kondo T, Takami T, Takahashi H, Ikuta H, Mizutani U, Funahashi R, Shikano M, Mikami M, Tsuda S, Yokoya T, Shin S and Muro T 2004 *Phys. Rev.* B **69** 125410